

## Supporting Information

for *Adv. Mater. Interfaces*, DOI: 10.1002/admi.202202456

Effects of the Polymer Amount and pH on Proton  
Transport in Mesopores

*Laura Despot and Annette Andrieu-Brunsen\**

Supporting Information

**Effects of the polymer amount and pH on proton transport in mesopores**

*Laura Despot, Annette Andrieu-Brunsen\**

Ernst-Berl-Institut für Technische und Makromolekulare Chemie, Technische Universität

Darmstadt, 64289 Darmstadt, Germany

E-mail: [annette.andrieu-brunsen@tu-darmstadt.de](mailto:annette.andrieu-brunsen@tu-darmstadt.de)

Thickness and refractive index of mesoporous silicafilms were determined in a series of 10 samples resulting in a mean film thickness of 565 nm $\pm$ 15 nm and a mean refractive index of 1.168 $\pm$ 0.007 (Table S1). A mean porosity of 62 vol.% $\pm$ 2 vol.% was calculated using the Bruggeman effective medium theory.<sup>[20]</sup>

**Table S1.** Ellipsometry measurements (RH=15 %) showing the film thickness d and refractive indices n of mesoporous silica films using fitting limits of 400-600 nm for film thickness and 1.0-1.5 for refractive index. In addition, the porosity calculated via the Bruggeman effective medium theory is listed.<sup>[20]</sup> Data presented as fitted film thickness/refractive index  $\pm$  error calculated for the respective parameter EP4-Model (version 1.2.0) from Accurion.

No.	d [nm]	n [a.u.]	RMSE	Porosity [vol.%]
1	561 $\pm$ 3	1.161 $\pm$ 0.003	1.469	63 $\pm$ 1
2	579 $\pm$ 4	1.175 $\pm$ 0.003	1.771	60 $\pm$ 1
3	566 $\pm$ 3	1.170 $\pm$ 0.003	1.572	61 $\pm$ 1
4	568 $\pm$ 3	1.170 $\pm$ 0.003	1.605	61 $\pm$ 1
5	561 $\pm$ 3	1.163 $\pm$ 0.003	1.472	63 $\pm$ 1
6	573 $\pm$ 3	1.173 $\pm$ 0.003	1.680	61 $\pm$ 1
7	552 $\pm$ 3	1.162 $\pm$ 0.003	1.409	63 $\pm$ 1
8	559 $\pm$ 3	1.169 $\pm$ 0.003	1.514	62 $\pm$ 1
9	575 $\pm$ 4	1.173 $\pm$ 0.003	1.757	61 $\pm$ 1
10	552 $\pm$ 3	1.163 $\pm$ 0.003	1.379	63 $\pm$ 1

Using the TEM image in Figure 1 a statistic pore size distribution of  $12.0 \pm 1.1$  nm representing the narrower part of the pore was determined.

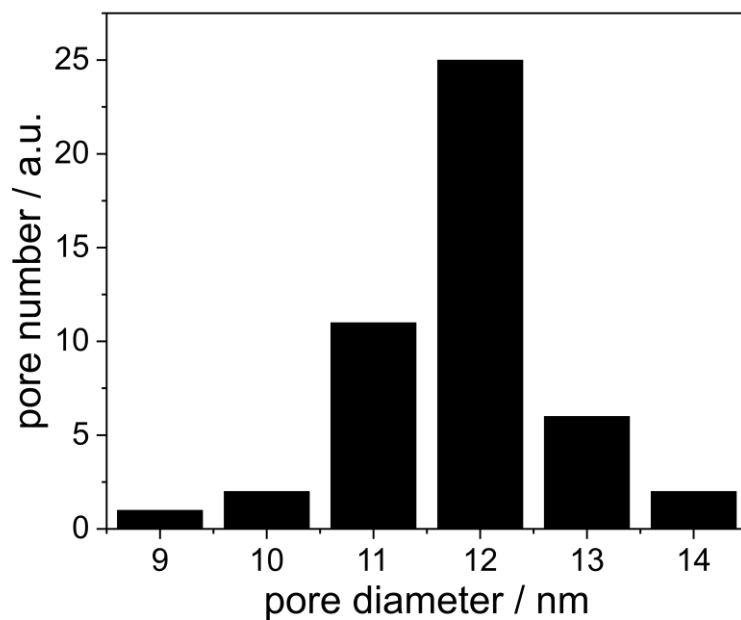


**Figure S1.** a) Statistic pore size distribution of a mesoporous silica film prepared by dip-coating (an average pore neck diameter of  $12.0 \pm 1.1$  nm was extracted from TEM image in Figure 1).

The UV-VIS-spectra of CDTPA in H<sub>2</sub>O:EtOH (1:7) show an absorption at around 450 nm wavelength (Figure S2). This is overlapping with the irradiation of visible light at 440-550 nm of the used light source.

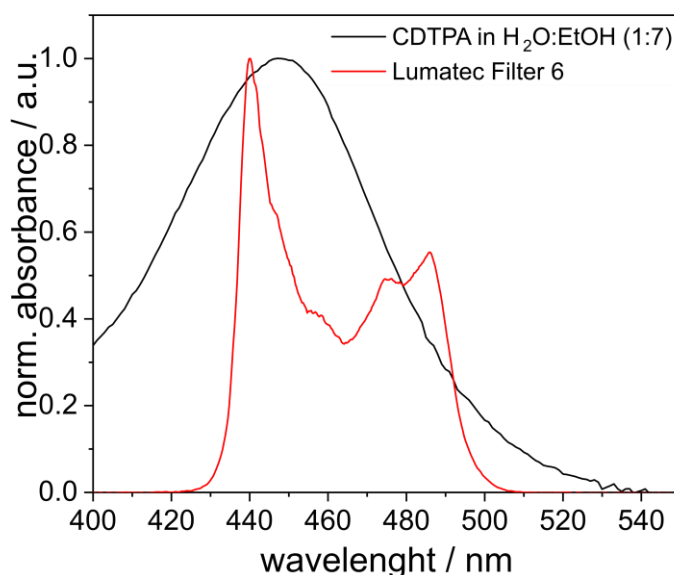


**Figure S2.** UV-Vis spectra of used filter of Lumatec lamp and CDTPA in H<sub>2</sub>O:EtOH (1:7).

The polymerization of SPMAC in solution was investigated using NMR spectroscopy. The monomer conversion (Figure S3b) indicates an almost linear increase of polymer chain length with irradiation time up to 1 h. After polymerization time of 1 h, the polymer quantity increases slower.

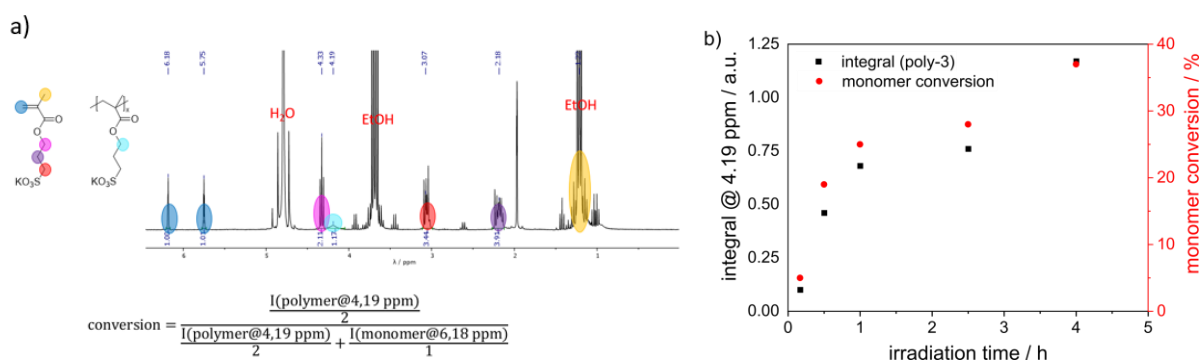


**Figure S3.** a) NMR spectra of polymerization solution after 4 h of irradiation with allocation of signals and equation to get monomer conversion. b) Integrals in NMR spectra of polymerisation solution at 4.19 ppm and monomer conversion, that are calculated according to equation on the left, are plotted against polymerization time

TEM and SEM images before and after light induced polymerization (Figure S4). The images show no significant changes in film thickness and pore structure indicating an intact porous silica film after polymerization.

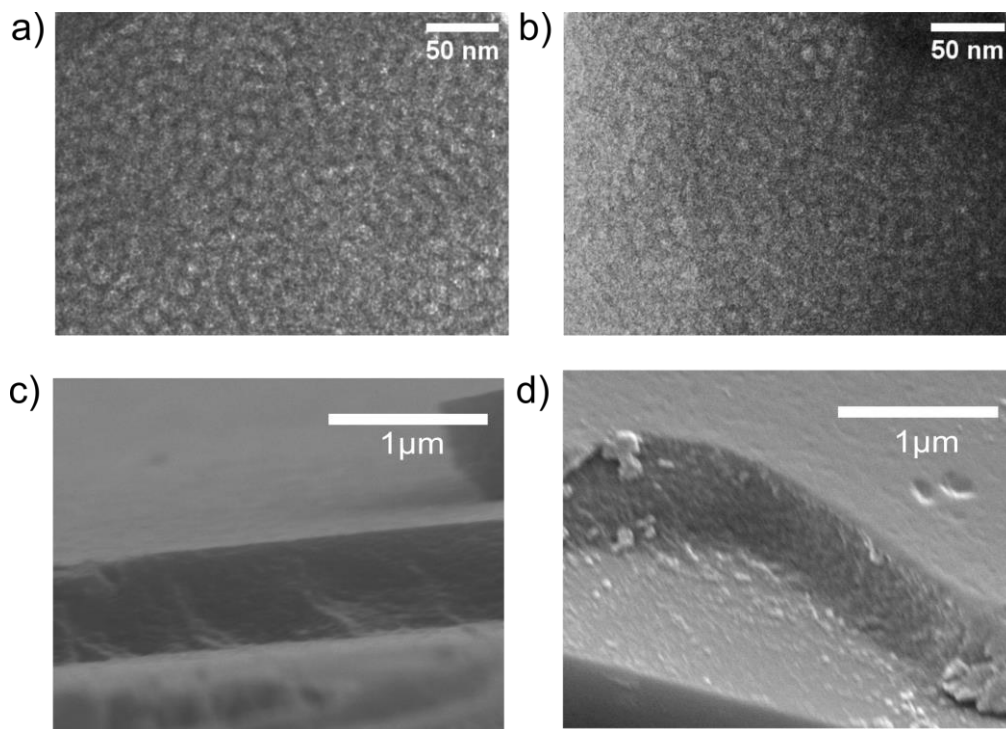


**Figure S4.** TEM images of mesoporous silica thin film before (a) and after (b) light induced polymerization of SPMAK of 2.5 h and SEM images before (c) and after (d) light induced polymerization of SPMAK of 2.5 h.

Polymer weight fraction and temperature stability were determined using TGA (Figure S5). Unfunctionalized (Figure S5a), allyltriethoxysilane functionalized (Figure S5b) and PSPMA functionalized silica films (Figure S5c-e) were analyzed. Polymer amount of 3 wt.% (Figure S5c), 6 wt.% (Figure S5d) and 22 wt.% (Figure S5e) were achieved.

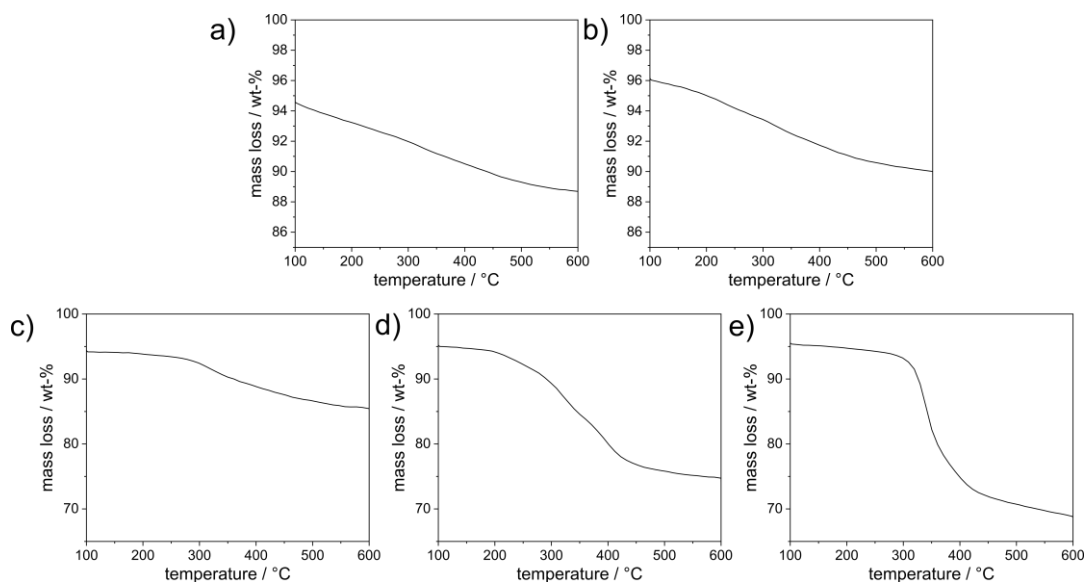


**Figure S5.** Determination of polymer fraction by thermogravimetric analysis. TGA mass loss of scratched off unmodified silica film (a), allyltriethoxysilane modified silica film (b) and PSPMA modified silica films with irradiation time of 10 min (c), 1 h (d) and 2.5 h (e).

To investigate the chemical stability of PSPMA bound to the pore surface IR measurements of the sample before and after incubating in nine aqueous solutions with different pH values were carried out. Incubation was carried out from the most acidic solution with a pH value of 1 to the most basic pH value of 10 for 5 min each. In between changing the solution, the sample was rinsed with water. HCl and NaOH were used to adjust the pH values. IR spectra show a slight variation of the C=O vibrational band at  $1710\text{ cm}^{-1}$  which is within the overall error of the experiment when measuring different positions on one sample (Figure S6). Consequently, no significant instability or loss of polymer was observed during EIS measurements.

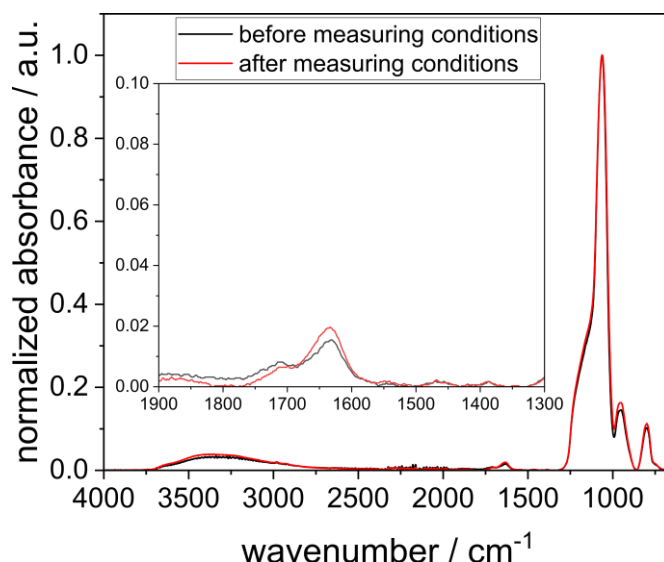


**Figure S6.** Normalized ATR-IR spectra of scratched off PSPMA functionalized silica films before and after incubation according to impedance spectroscopy measurement conditions. Difference in intensities of C=O vibration lays within the overall error.

Temperature dependent impedance measurements were performed between 30 °C and 60 °C at a neutral solution pH using an unfunctionalized and a PSPMA functionalized mesoporous silica film after polymerization time of 1 h resulting in 15 wt.% PSPMA. It is shown in Figure S7a that with increasing temperature the proton conductivity is increasing as the mobility of conducting species increases with temperature. The activation Energy  $E_a$  was calculated using the Arrhenius equation  $\sigma = \sigma_0 \exp(E_a/k_b T)$ , where  $\sigma$  is the proton conductivity,  $\sigma_0$  the pre-exponential factor and  $k_b$  the Boltzmann's constant. Activation energies of 0.19 eV for the unfunctionalized silica film and 0.14 eV for the PSPMA functionalized silica film were obtained (Figure S7b). Typical activation energies of the Grotthuss mechanism lay in a range of 0.14 – 0.40 eV.<sup>[1]</sup> suggesting that the primary mechanism for proton transport using mesoporous silica films is the Grotthuss mechanism. This meets our expectations as  $E_a$  of 0.11 to 0.26 eV were reported for sulfonic acid functionalized mesoporous silica.<sup>[2, 3]</sup> In comparison, the  $E_a$  of Nafion has been reported as 0.1 to 0.2 eV.<sup>[4, 5]</sup>



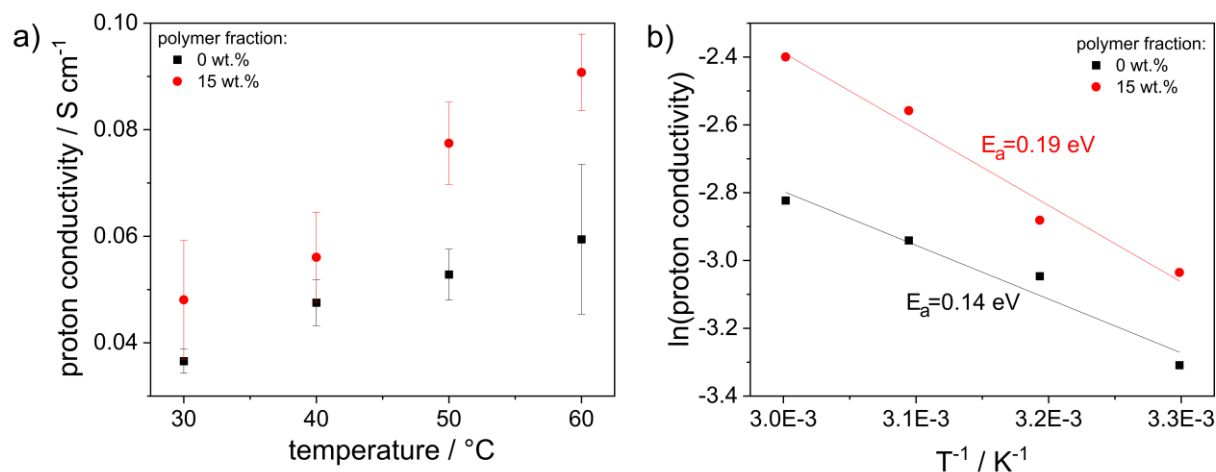


**Figure S7.** a) Proton conductivity of an unfunctionalized and a PSPMA functionalized mesoporous silica film against temperature at neutral solution pH. Proton conductivity was calculated by  $\sigma=L/RA$  using fitted resistances and sample and set-up dimensions. Data presented as calculated proton conductivity  $\pm$  error calculated via propagation of uncertainty using the errors from fitting impedance data using RelaxIS 3 from rhd instruments. b) Arrhenius plots of the conductivities and the obtained activation energies.

PH dependent EIS measurements of two independently fabricated unfunctionalized silica films show the reproducibility of the measurement (Figure S8a). Incorporating PSPMA into the pores leads to decreasing resistance with increasing polymer amount (Figure S8b).

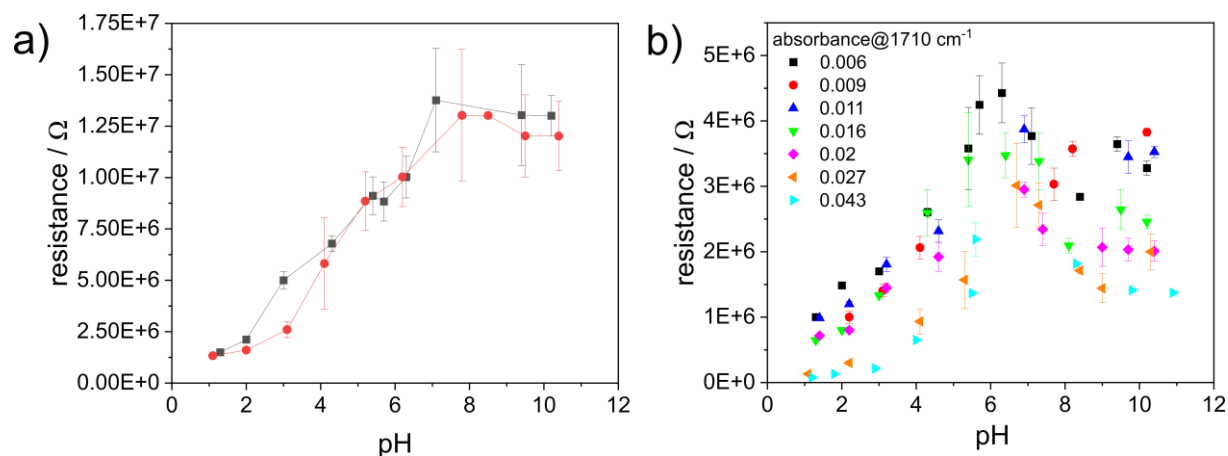


**Figure S8.** a) Fitted resistances of two independent mesoporous silica films on ITO electrode against pH of the surrounding solution. Data presented as fitted resistance  $\pm$  error calculated for the parameter using RelaxIS 3 from rhd instruments. b) Fitted resistances of PSPMA functionalized mesoporous silica films on ITO electrode with different polymer amounts indicated by the C=O absorbance at 1710 cm<sup>-1</sup> against pH of the surrounding solution. Data presented as fitted resistance  $\pm$  error calculated for the parameter using RelaxIS 3 from rhd instruments.

### Cyclic voltammetry studies

Cyclic voltammetry was used for studying pH-dependent proton transport. Due to silanol groups of the mesoporous silica film and the sulfonic acid groups of the polymer a change of the solution pH from acidic to basic leads to an increase in negative charge inside the pores and thus to electrostatic attraction between the pore and a cationic probe molecule. This is reflected in an increase of the peak current density in the cyclic voltammograms.

Measurements were performed while changing the pH from 3.0 to 10.2. Peak current densities were plotted against the solution pH as seen for a PSPMA silica film in Figure S9a. The data points were subjected to an empirical Boltzmann-fit whereas the turning point is assigned to the pKa value of the PSPMA modification (Figure S9b) or the silanol groups of the mesoporous silica film (Figure S9c).

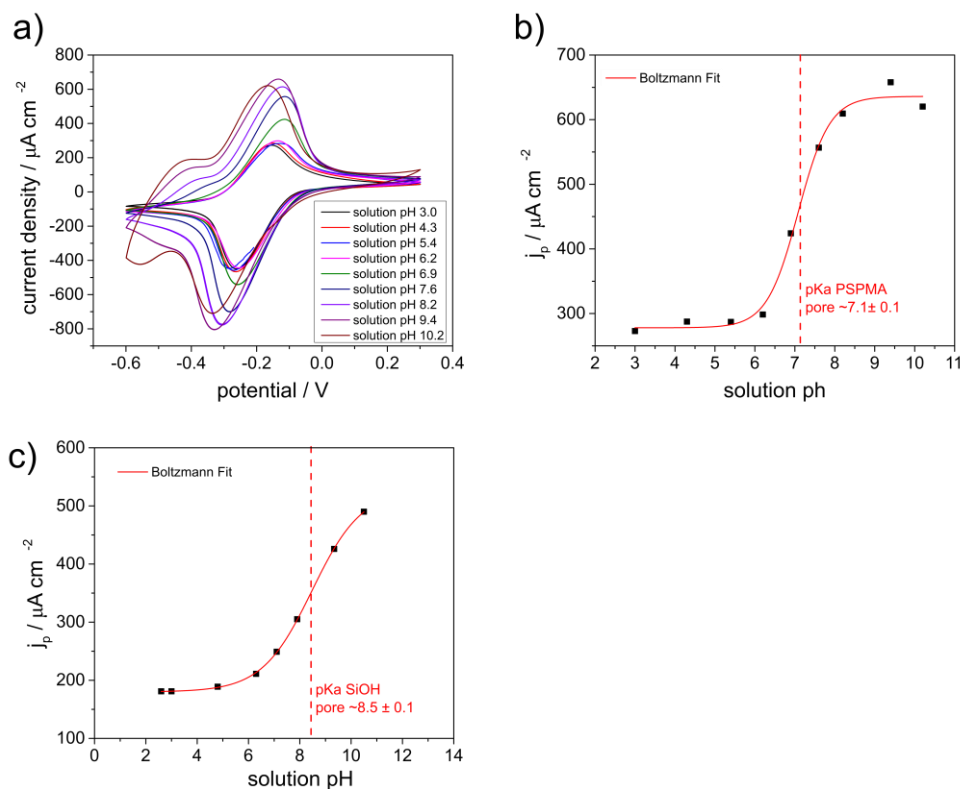


**Figure S9.** a) Cyclic voltammograms of a PSPMA modified mesoporous silica film at different pH values using  $10^{-3}$  M  $[\text{Ru}(\text{NH}_3)_6]^{2+/3+}$  as probe molecule in phosphate buffer solution. Scanrate  $100 \text{ mV s}^{-1}$ . b) Peak current density values ( $j_p$ ) plotted against the measurement solution pH using PSPMA functionalized silica film on ITO substrate.  $\text{pK}_a$  value, obtained from Boltzmann-fit, indicated with red dashed line. c) Peak current density values ( $j_p$ ) plotted against the measurement solution pH using mesoporous silica film on ITO substrate.  $\text{pK}_a$  value, obtained from Boltzmann-fit, indicated with red dashed line.

To investigate the permselectivity of a PSPMA functionalized mesoporous silica film cyclic voltammetry measurements were performed at acidic and basic pH using a cationic ( $[\text{Fe}(\text{CN})_6]^{3-/4-}$ ) and an anionic probe molecule ( $[\text{Ru}(\text{NH}_3)_6]^{2+/3+}$ ) shown in Figure S10. When changing from acidic to basic solution pH an increase of peak current density is seen. This is a result of the deprotonation of the sulfonic acid groups and generating a negatively charged pore surface. Therefore, electrostatic attraction between the positively charged probe molecule and the negatively charged sulfonic acid groups occur. Using the anionic probe molecule only a very low peak current density is detected, which indicates an exclusion of the negative charged probe molecule from the mesopores. Even at an acidic pH, sufficient sulfonic acid groups seem to be deprotonated resulting into electrostatic repulsion of the negatively charged probe molecule.

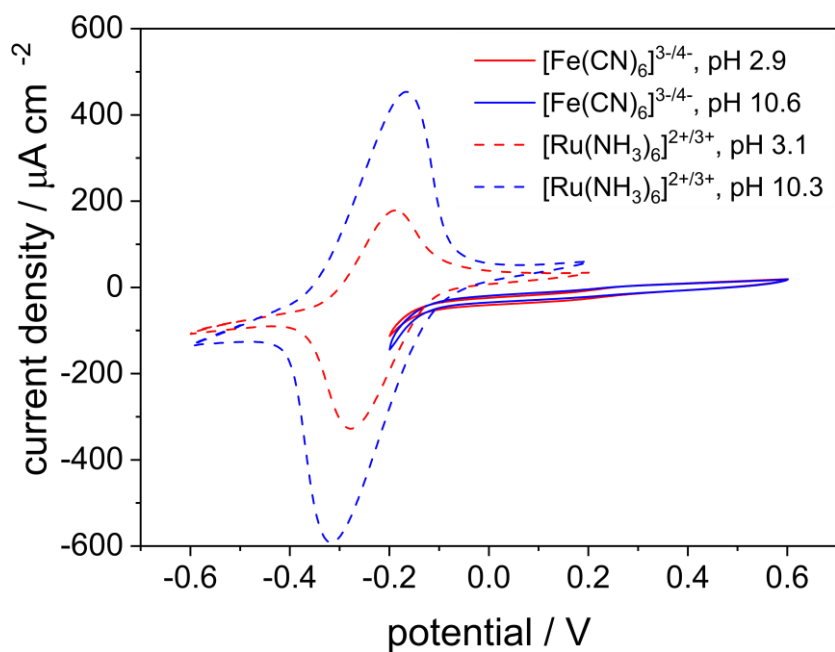


**Figure S10.** Cyclic voltammograms of a PSPMA modified mesoporous silica film (9 wt.% of PSPMA) at basic and acidic pH values using  $10^{-3}$  M  $[\text{Ru}(\text{NH}_3)_6]^{2+/3+}$  and  $[\text{Fe}(\text{CN})_6]^{3-/4-}$   $10^{-3}$  M as probe molecule in 0.1 M aqueous KCl solution. Scanrate  $100 \text{ mV s}^{-1}$ .

Figure S11 show EIS measurements at neutral solution pH. An increase of PSPMA leads to an increase of the proton conductivity from 0.013 to 0.026 S cm<sup>-1</sup>.

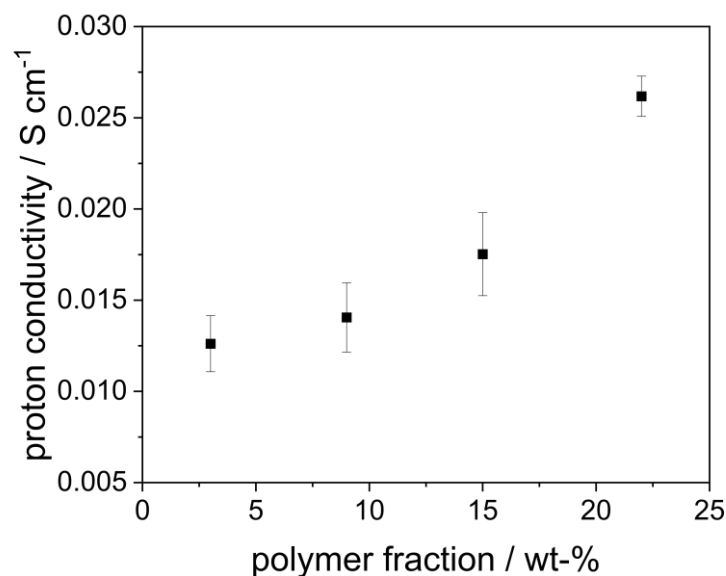


**Figure S11.** Proton conductivity of PSPMA functionalized mesoporous silica film against the irradiation time and therefore the polymer content at neutral solution pH. Proton conductivity was calculated by  $\sigma=L/RA$  using fitted resistances and sample and set-up dimensions. Data presented as calculated proton conductivity  $\pm$  error calculated via propagation of uncertainty using the errors from fitting impedance data using RelaxIS 3 from rhd instruments.

Figure S12 presents the Nyquist (imaginary part of impedance  $-Z''$  vs real part  $Z'$ ) of an unfunctionalized mesoporous silica thin film and PSPMA functionalized mesoporous silica films with increasing polymer amount at acidic solution pH (Figure S11a) and basic solution pH (Figure S11b). The impedance spectra of PSPMA functionalized silica films measured at basic solution pH (Figure S11b) show three semicircles. The EC used to fit the data thus consists of three time constants. The surrounding solution is represented by an EC including a parallel resistance  $R_s$  and capacitor  $C_s$ . The porous silica film is represented by a pore resistance  $R_{\text{pore}}$  with a constant phase element  $\text{CPE}_{\text{dl}}$  and a parallel polymer resistance  $R_{\text{polymer}}$  in a row and an additional pore wall capacitor  $C_{\text{pore wall}}$  in parallel. For the unfunctionalized and allyl-functionalized silica films  $R_{\text{polymer}}$  and  $\text{CPE}_{\text{dl}}$  were excluded. The EC for fitting remains constant for impedance measurements as the overall measuring set up is not changing when changing the solution pH. The impedance spectra at basic and acidic pH show a

decreasing slope at low frequencies when PSPMA amount increases. This results in a decreasing resistance and increasing proton conductivity as it is described in Figure 4.

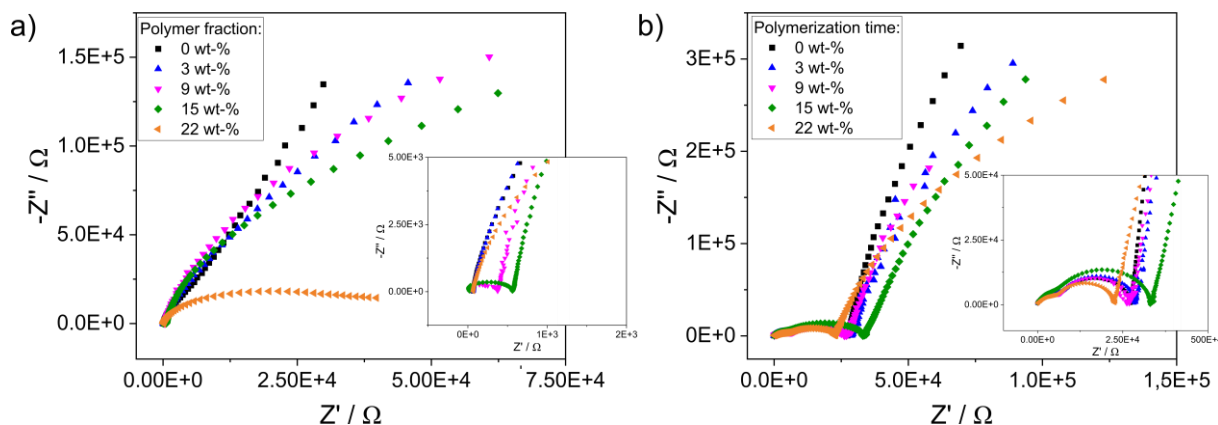


**Figure S12.** Nyquist plots of PSPMA functionalized mesoporous silica films on ITO electrode with different polymer amounts indicated by the polymerization time. EIS were measured at acidic (a) and basic (b) solution pH.

## References

- [1] Y. Ren, G. H. Chia, Z. Gao, *Nano Today* **2013**, 8, 577-597.
- [2] S. Fujita, A. Koiwai, M. Kawasumi, S. Inagaki, *Chem. Mater.* **2013**, 25, 1584–1591.
- [3] I. S. Amiin, X. Liang, Z. Tu, H. Zhang, J. Feng, Z. Wan, M. Pan, *ACS Appl. Mater. Interfaces* **2013**, 5, 11535–11543.
- [4] M. Cappadonia, J. W. Erning, S. M. S. Niaki, U. Stimming, *Solid State Ionics* **1995**, 77, 65-697.
- [5] S. Feng, G. A. Voth, *J. Phys. Chem. B* **2011**, 115, 19, 5903–5912.